Preferred citation: A. Jäsberg, P. Selenius and A. Koponen. The effect of fibrous materials on the rheology of aqueous foams. In **Advances in Pulp and Paper Research, Oxford 2017**, *Trans. of the XVIth Fund. Res. Symp. Oxford, 2017*, (W. Batchelor and D. Söderberg, eds), pp 159–173, FRC, Manchester, 2018. DOI: 10.15376/frc.2017.1.159.

THE EFFECT OF FIBROUS MATERIALS ON THE RHEOLOGY OF AQUEOUS FOAMS

Ari Jäsberg, Pasi Selenius and Antti Koponen

VTT Technical Research Centre of Finland Ltd
P.O. Box 1000, FI-02044 VTT, Finland
Ari.Jasberg@vtt.fi

ABSTRACT

We studied fully developed pipe flow of fibre-laden aqueous foams and decoupled their bulk rheological properties from boundary effects like slippage at the pipe wall. The air volume fraction of the foams varied between 70% and 75%. The addition of hardwood fibres at consistency 20 g/kg to plain aqueous foam increased viscosity more than 100%, while with microfibrillated cellulose at a consistency of 25 g/kg the increase was about 30%. The effect of synthetic (cellulosic) rayon fibres was negligible at the consistency of 20 g/kg. All the studied foams could be described as shear-thinning power-law fluids with significant slippage at the pipe wall. The differences in flow behaviour could be explained by particle size and interactions between particles and bubbles.

INTRODUCTION

In the 1970s several articles on foam, as a replacement for water in paper making, were published [1–3]. In this process, an aqueous viscous foam is used to transport fibres and to deposit them via a drainage process. Foam-forming aroused interest, as the movement of fibres is restricted in the foam while flocculation is reduced – this gives the web outstanding uniformity. In the mid-70s a few

pilot paper machines utilising foam-forming were indeed run rather successfully, but it was not widely adopted in the paper industry. The process was later further developed for the nonwoven industry for transport of polymeric, metal, glass and other mineral fibres, and is nowadays used for making various nonwoven products.

After a long silent period, foam-coating [4, 5] and foam-forming are now attracting increasing interest in the paper industry [6–11]. The use of foam allows the inclusion of a wide variety of alternative raw materials, such as nanoparticles [12], nanocellulose [13] and long flexible fibres [14]. This technique will also lead to more versatile production methods that are required for manufacturing new types of end products, such as high-porosity cellulose nanofibril (MFC) aerogels [15]. Naturally, energy efficient technologies are presently also of interest due to rising energy costs, and with foam-based techniques in papermaking, water consumption is reduced and less energy is needed in drying.

In all of those new applications, the rheology of the foam must be tuned to meet the requirements of the product or process. However, although rheology of plain aqueous foams has been studied extensively, particle-foam systems have got much less attention [16]. Moreover, there is almost no information available on the rheological behaviour of fibre-laden foams [17]. Systems of fibres and gas bubbles have been studied in relation to the flotation process both in the mining and paper industry [18], but almost all publicly available results on pure fibre-laden foams can be found in patents for producing nonwoven products. There is thus an urgent need for fundamental research on the underlying physics and physical chemistry of fibre-laden foams.

Due to problems related to the ageing of foam and often strong slip flow at solid boundaries, rheological analysis of liquid foams is not feasible with most traditional rheometer geometries. Instead, pipe flow has mainly been used, and the effect of slip has been determined with Mooney analysis, i.e. by assuming

$$v_s = \frac{\beta \tau_w}{D}, \tag{1}$$

where υ_s is the slip velocity, τ_w is the wall shear stress, and D is pipe diameter. The dependence of coefficient β on the wall shear stress is then determined by performing the measurements with several different pipe diameters [19, 20]. In this work, we will measure the slip velocity directly by using high-speed imaging. Most previous studies have concentrated on dry foams. Furthermore, the air content of the foam is that of a typical foam foaming process, i.e. 70 % – we are thus in the wet foam regime [21].

MATERIALS AND METHODS

Experimental setup

The measurements were carried out with a glass pipe with a diameter of 15 mm and length of 2.0 m. Differential pressure transducers were used to measure both the pressure drop over a 1.0 m long measurement section as well as the gauge pressure at the end of the measurement section. A magnetic flow meter measured the volumetric flow rate at a position that was close to pipe exit; the pressure at the measurement point was thus close to the atmospheric pressure. At the pipe exit, the flow discharged into a container standing on a scale, which recorded the cumulative mass flow. A high-speed video (HSV) camera was used in the measurement section to record foam motion at the pipe wall. The HSV camera recorded the foam surface at the frame rate of 1000 fps with a spatial resolution of 12 μm/pixel. The resolution of the HSV sensor was 1280 × 1024, giving the maximum imaging area of 15.4 mm × 12.3 mm.

All foams were generated with a combination of tank mixing and inline generation in a short flow loop, see Figure 2. The tank mixer has been specifically designed for foam generation and it has three round impeller plates with opposite edges slightly bent up and down [7]. The inline generation was implemented by

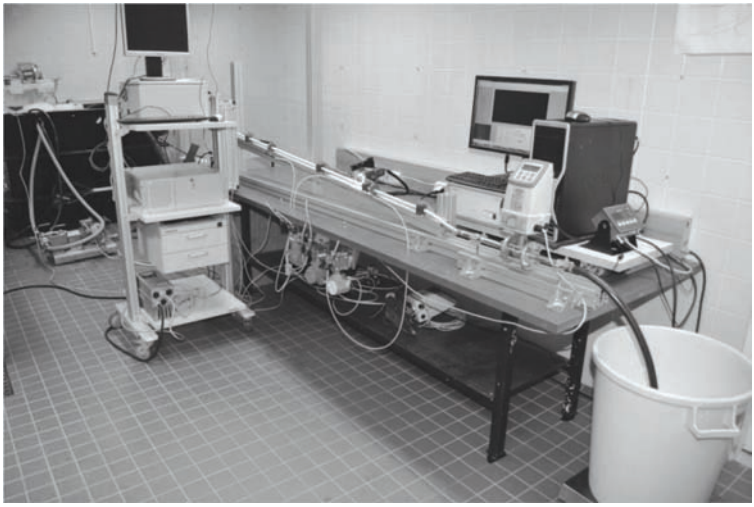

Figure 1. A photograph of the experimental setup. To the left is the 300 l tank used for foam generation and storage; in the middle is the measurement pipe equipped with differential pressure transducers, magnetic flow rate meter, and high-speed video camera; to the right, the flow discharges into a vessel standing on a scale measuring mass flow rate.

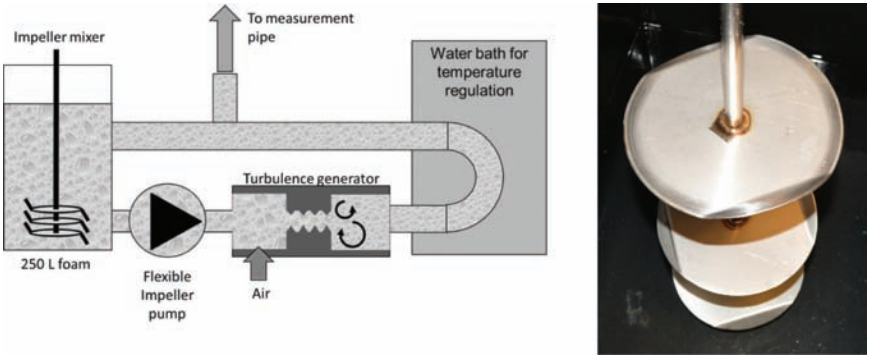

Figure 2. Left: schematic view of the foam generation setup. Right: the three-blade impeller used for foam generation.

injecting compressed air into the SDS solution in a specifically designed inline generation block where the flow field is highly turbulent.

The foam generation phase was started by adding the Sodium dodecyl sulfate (SDS) solution into the tank, followed by mixing and air injected into the solution until the target value of foam density was reached (given by the surface level of the foam inside the tank). During the measurements, the air content and bubble size of the foam was stabilised before measurements by pumping it continuously through the inline generation block (without air injection), and by mixing the foam inside the tank to minimise density gradients due to foam drainage. In the setup used in this study, the majority of the pumping power is dissipated into heat by viscosity in the turbulent flow field inside the generation block, which manifests itself by a high-pressure drop over the block. The foam temperature was regulated (usually 25 °C) by making it flow through a steel pipe section immersed into a bath of cooling water. During the measurements, a two-way valve in the return pipe (after the inline generation block and the cooling bath) was adjusted to have a selected mass flow rate of boosted foam to flow into to the measurement pipe.

Materials

The measurements were carried out by using aqueous foams with and without added fibres. Aqueous foams were generated from a solution of tap water and anionic surfactant sodium dodecyl sulphate (SDS, $C_{12}H_{25}SO_4Na$). Fibre-laden foams were prepared by adding fibres into the initial SDS solution. The molar concentration of the SDS solution used in this study was 8.5 mM, which is above the critical micelle concentration 8.2 mM. The amount of SDS solution used for

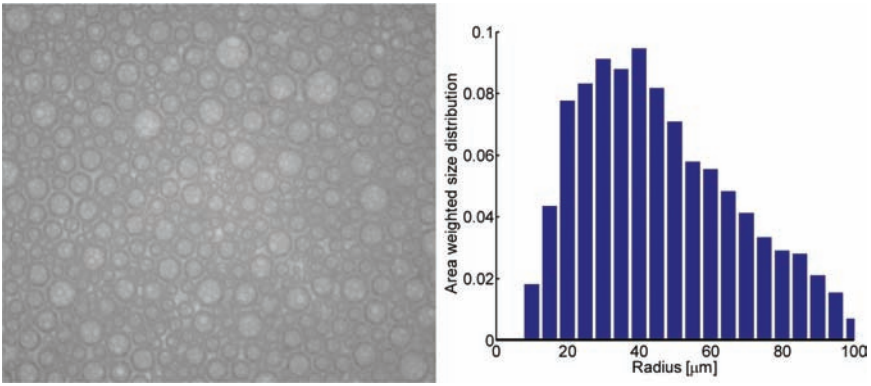

Figure 3. Left: a microscopic image (2 mm × 2 mm) of an aqueous foam sample taken from the mixing tank (temperature 38°C and density 310 g/l) in a 1 mm thick slab between two glass plates. Right: bubble size distribution of the foam sample as calculated from a set of six such images. In this case, the mean bubble radius is 47 μm.

one batch was 80 litres, and the density of the generated foam varied from 250 g/l to 310 g/l, i.e. the volumetric liquid fraction varied from 0.25 to 0.31. The half-life of foam was measured for offline samples taken from the mixing tank, and it decreased with increasing density. For the foams used in this study, the half-life varied between 4 and 5.5 minutes. The bubble size distribution of the offline samples was determined from microscopic images in a narrow slab between two glass plates by using the method and algorithm described in the reference [22]. It was found that the mean bubble size increased with increasing density and temperature. An example image of an offline foam sample taken from the mixing tank and its bubble size distribution are shown in Figure 3. The size distribution is weighted by the bubble frontal area $\pi\alpha^2$, thus each bar in the graph gives the share of the total bubble area in the image.

Wood fibre-laden foams were prepared by adding chemically released hardwood (birch) fibres to the SDS solution at the fibre consistency of 20 g/kg. These cellulose fibres are elongated slender bodies with characteristic length of ca. 1 mm (10 times the mean bubble diameter) and characteristic width of ca. 15–20 μm (15–20% of the mean bubble diameter), see Figure 4. The qualitative effect of fibre morphology was tested by studying aqueous foam with synthetic rayon fibres at the same consistency 20 g/kg. The rayon fibres used in this study are relatively straight cylindrical rods with smooth hydrophilic surface, and their length and diameter are close to those of the hardwood fibres. In addition, the qualitative effect of fibre dimensions was tested by studying aqueous foam with microfibrillated cellulose (MFC) at consistency 25 g/kg.

Figure 4. Microscopic images of hardwood fibres (left) and synthetic rayon fibres (middle) used in this study. The width of the fibre images is 1.5 mm. The length of rayon fibres is 1 mm, i.e. approximately equal to the mean length of hardwood fibres. At the right is a SEM image of the MFC grade used in this study (Celish® KY-100G, Daicel Chemical Industries, Japan).

In fibre suspension analysis, the effective rheological concentration is often estimated with the crowding number n_f, which is the average number of fibres that are inside a sphere whose diameter is equal to the average fibre length [23]. It can be calculated from the formula $n_f = \pi c L^2/6w$, where c is the consistency of the pulp, L is average fibre length, and w is the coarseness of the fibres defined as mass per unit length. Kerekes and Schell [24] determined the following three regions for n_f: when $n_f < 1$ fibres will only have random contact, when $1 < n_f < 60$ fibres have forced collisions in shear, and when $n_f > 60$ the fibres are in continuous contact. The crowding number using the reduced effective consistency $c(1 - \phi)$ for the hardwood fibre-laden foam (with the air content of $\phi = 0.7$, and coarseness of $w = 0.11$ mg/m) is in our case 33. The fibres are thus in continuous contact in shear flow.

Data analysis

In stationary flow in a circular pipe the wall shear stress is independent of the detailed flow profile and can be calculated from the measured pressure drop per unit length:

$$\tau_w = \frac{D}{4}\frac{dP}{dL}. \tag{2}$$

In order to extract material parameters, one has to examine the foam in the frame of reference moving at the speed of the slip velocity. To that end, the slip velocity is subtracted from the mean flow velocity

$$\tilde{v}_{\text{bulk}} = v_{\text{avg}} - v_s. \tag{3}$$

Apparent foam shear rate $\dot{\gamma}_a$ at the edge of the foam plug is defined as

$$\dot{\gamma}_{\alpha} = \frac{8\tilde{v}_{\text{bulk}}}{D}, \tag{4}$$

where D is the inner diameter of the pipe. The real shear rate $\dot{\gamma}$ at the pipe wall can now be obtained by applying the Weissenberg-Rabinowitsch correction that takes into account the non-Newtonian features of the velocity profile [25, 26]:

$$\dot{\gamma} = \dot{\gamma}_{\alpha} \times \frac{1}{4}\left(3 + \frac{d\ln\dot{\gamma}_{a}}{d\ln\tau_{w}}\right). \tag{5}$$

Viscosity with a given shear rate is now obtained as the ratio of the wall shear stress to the real wall shear rate:

$$\mu = \tau_{w}/\dot{\gamma}. \tag{6}$$

RESULTS

In Figure 5 the flow loss curve (i.e. the measured pressure drop per unit length in the pipe flow as a function of mean flow rate) is shown for plain aqueous foam at

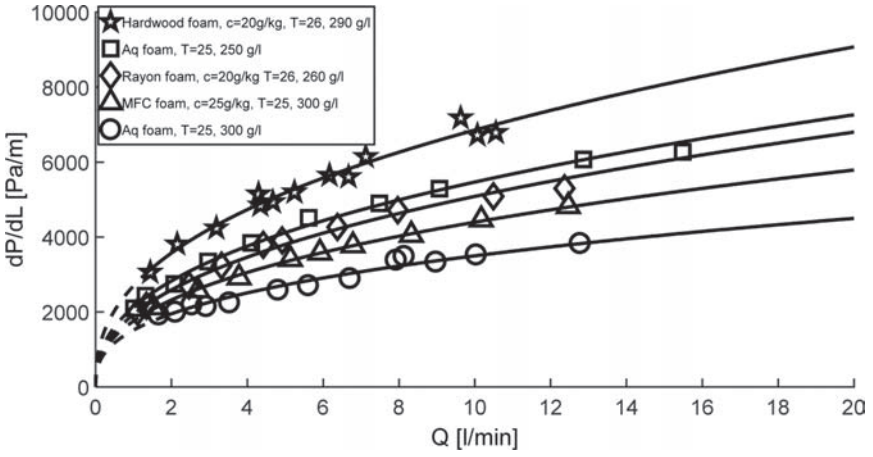

Figure 5. The measured pressure drop vs. flow rate for aqueous foam at two different densities, and for three fibre-laden aqueous foams. Solid lines are a least-squares fit of power-law Eq. (7) to the measured data. Dashed lines are the fits plotted in the low flow-rate regime with no valid experimental data.

two different densities (circle and square markers) and for three fibre-laden aqueous foams. We see that the flow behaviour of all the foams is shear-thinning. It can also be seen that the loss in aqueous foam increases with decreasing density. By comparing the loss in hardwood fibre-laden foam (star markers) to the loss in corresponding plain aqueous foam (circle markers, nearly at the same density), one finds that the addition of fibres increases the loss approximately by a factor of two. The addition of MFC at consistency 25 g/kg (triangle markers) leads to ca. 25% increase in the pressure loss, whereas the effect of rayon fibres at consistency 20 g/kg is negligible. It will be shown below that the flow behaviour seen in Figure 5 is a combined effect of the wall slip and shearing of the foam plug. At very low flow rates foam moves as rigid plug and all shearing takes place in the slip layer next to the pipe wall, while at high flow rates, a considerable amount of shearing occurs inside the foam.

The measured slip velocity as a function of the wall shear stress is plotted in Figure 6. The slip increases in all cases with wall shear stress, as expected. At high wall shear stress the slip velocity increases with foam density; at low wall shear stress the effect of the density is relatively small. This is in agreement with the widely accepted view the slip velocity is due to a layer of pure liquid (solution of water and SDS in this study) forming at the pipe wall [27, 28]. By comparing the slip in the hardwood fibre-laden foam to the slip in the corresponding plain aqueous foam, one can see that at high shear stress the

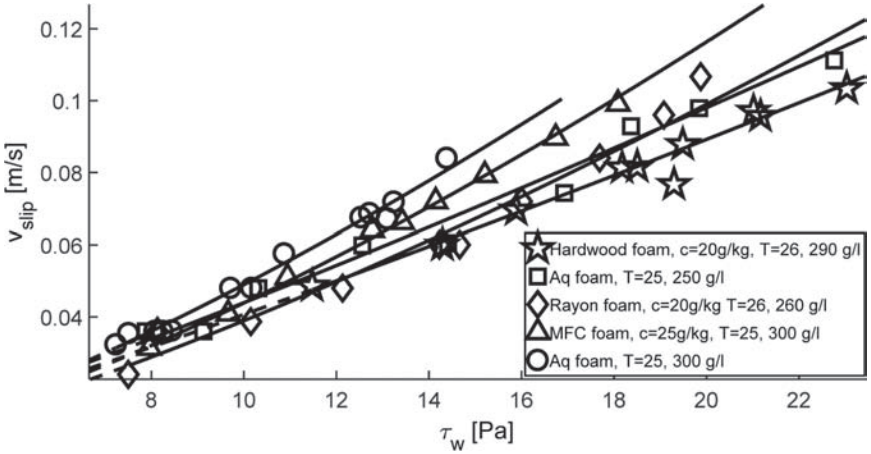

Figure 6. The measured slip velocity vs. the wall shear stress. Foams and plot markers are the same as in Figure 5. Solid lines are a least-square fit of power-law Eq. (8) to the measured data. Dashed lines are the fits plotted in the low flow-rate regime with no valid experimental data.

presence of fibres decreases the slip velocity by up to 30%. Moreover, the slip velocity in the fibre-laden foam at density 290 g/l is even smaller than in plain aqueous foam at density 250 g/l.

It was found that both the loss data, shown in Figure 5 and the slip velocity data, shown in Figure 6 follow closely power-law forms. We did least-squares fits of the following formulae to the measured data:

$$\frac{dP}{dL} = \beta_p v_{\text{avg}}^{n_p} \tag{7}$$

$$v_s = \beta_s \tau_w^{n_s} \tag{8}$$

The values of the fitted parameters are shown in Table 1. It can be seen that the slip velocity is a slightly nonlinear function of the wall shear stress. The constant β in Eq. (1) can be written in a form, $\beta = \beta_s \tau_w^{n_s - 1} D$, where the exponent of slip nonlinearity $n_s - 1$ varies between 0.13 and 0.40.

The relative slip velocity, i.e. the ratio of the slip velocity to the mean flow velocity, as a function of the wall shear stress is shown in Figure 7. The solid and dashed lines are calculated from Eqs (7) and (8) with the parameter values given in Table 1. The measured relative slip values are always smaller than 40%, i.e. considerable shearing takes place inside the foam. The relative slip increases with decreasing density, and the addition of fibres have a clear effect on the relative slip velocity; the relative slip in the fibre-laden foam (stars) is about four times the slip velocity in the corresponding plain aqueous foam (circles).

We finally turn to the rheological properties of the foam plug itself. We apply Eqs (3)–(5) to get the real shear rate and viscosity at the surface of the foam plug. The foam viscosity is shown in Figure 8 as a function of shear rate. The viscosity

Table 1. The values of the fitted parameters in Eqs (8) and (9)

	$\beta_p \left[\frac{\text{Pa}}{\text{m}}\left(\frac{m}{s}\right)^{-1}\right]^{-n_p}$		$\beta_s \left[\frac{\text{mm}}{\text{s}}\text{Pa}^{-n_s}\right]^{n_s}$	
Hardwood foam, c = 20g/kg, 290	2700 ± 100	0.40 ± 0.02	3.0 ± 0.4	1.13 ± 0.05 g/l
Rayon foam, c = 20 g/kg, 260 g/l	1940 ± 80	0.42 ± 0.02	1.8 ± 0.3	1.35 ± 0.05
MFC foam, c = 25 g/kg, 300 g/l	1760 ± 70	0.40 ± 0.02	1.7 ± 0.3	1.40 ± 0.05
Aq. foam 250 g/l	2130 ± 40	0.41 ± 0.01	3.1 ± 0.5	1.16 ± 0.07
Aq. foam 300 g/l	1520 ± 50	0.36 ± 0.02	2.1 ± 0.3	1.37 ± 0.05

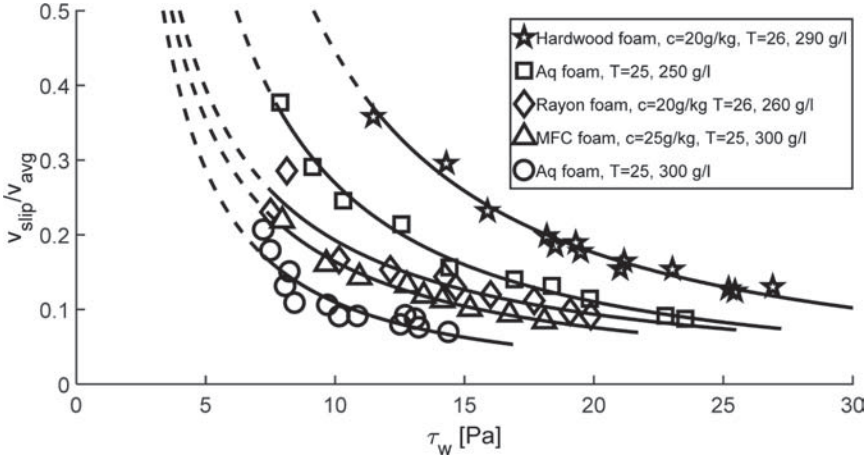

Figure 7. The relative slip velocity vs. wall shear stress. Foams and plot markers are the same as in Figure 5. The solid and dashed lines have been calculated starting with the fitted lines presented in Figures 5 and Figure 6, i.e. from Eqs (7) and (8).

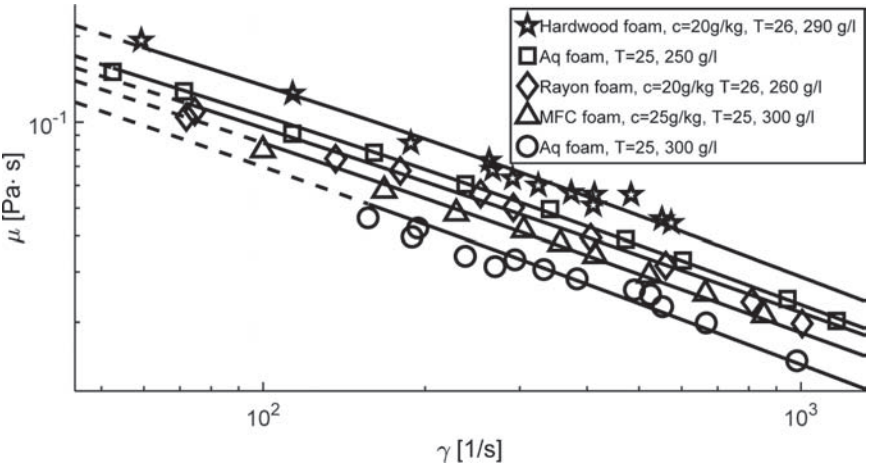

Figure 8. Viscosity vs. shear rate as given by Weissenberg-Rabinowitsch correction (5). Foams and plot markers are same as in Figure 6. The solid lines are calculated from Eq. (9), with the values in Table 2, and with $n = 0.6$.

Table 2. Fitted values of the consistency index k_0 for the fixed value n = 0.6 of the flow behaviour index

	k_0 [Pa·$s^{0.6}$]
Hardwood foam, c = 20g/kg, 290 g/l	0.66 ± 0.02
Rayon foam, c = 20 g/kg, 260 g/l	0.47 ± 0.03
MFC foam, c = 25 g/kg, 300 g/l	0.40 ± 0.03
Aq. foam 250 g/l	0.53 ± 0.02
Aq. foam 300 g/l	0.30 ± 0.02

increases with foam dryness and the addition of hardwood fibres at consistency 20 g/kg increases the viscosity by a factor of two.

It was found that the viscosity given by a power-law model

$$\mu = k_0 \dot{\gamma}^{n-1} \tag{9}$$

reproduces the experimental data with good accuracy. Considering the experimental error all the fitted values of the flow behaviour index n were in good agreement with value n = 0.6 (the average value was n = 0.61 ± 0.03). The fitted values of the consistency index k_0 with the fixed value n = 0.6 are shown in Table 2, and the corresponding viscosity calculated from Eq. (9) is shown as solid lines in Figure 8. It is important to notice that the fitted value n = 0.6 is different than the power-law index n_p of the loss data (see Table 1). This is due to the fact that the effect of the wall slippage is included in the loss data but it is removed from the viscosity data.

DISCUSSION

Viscosities of suspensions are often expressed with the relative shear viscosity, μ_r, which is obtained by dividing the suspension viscosity with the viscosity of the carrier fluid. There are several studies where the shear viscosity of water suspensions of smooth fibres have been carried out. In [29], e.g. a master curve is given, where the relative viscosity is presented as the function of nL^2d, where n is the number density of fibres, L is fibre length and d is fibre diameter. In our case, by using the reduced effective consistency, we get relative viscosities of 1.2 and 1.6 for the rayon suspension and the hardwood suspension, respectively. So, the effect of rayon on the foam viscosity is much smaller than on water. This may be due to two factors: the interaction between the bubbles and rayon fibres is weak, and the fibre-fibre interactions are restricted by the bubbles. More work is obviously needed here. For hardwood, the effect of fibres on viscosity is bigger in foam than that of smooth fibres in water, which is likely caused by their rough surfaces which increase the

strength of fibre-fibre and fibre-bubble interactions. Indeed as Figure 9 shows, bubbles tend to attach to the surfaces of the natural fibres.

The flow properties of plain aqueous suspensions of various wood fibres have been studied extensively in the past. In the studies with fibres having similar characteristics to the hardwood fibres used here and at the same fibre consistency, the apparent viscosity (in the laminar flow regime) has been found to be higher than that of water by a factor five or even more [30]. This is much more than for a similar suspension of smooth fibres (see above). Moreover, in this study, we observed the addition of fibres to increase the shear viscosity of foam only by a factor of two. We can thus conclude that in aqueous foams fibres do not interact with each other or flocculate to the same extent as in plain aqueous suspensions. The bubble curtain surrounding the fibres (see Figure 9) tends to prevent direct collisions between the fibres. This result is in accord with the fact that paper samples created by using foam forming technology have generally much better formation (smaller fibre flocs) than the samples created with traditional water forming [8].

The viscosity of Daicel foam is approximately the same (the difference is less than 20%) as was obtained in an earlier study for water-Daicel suspensions [31]. It seems that the dampening of MFC flocculation due to bubbles is in this case fully compensated with the increased dissipation on bubble surfaces.

The result for the relative slip in Figure 7 indicates that the relative slip might reach 100% at non-zero wall shear stress, i.e. below this yield stress foam moves as a rigid plug. This speculation is supported by a careful inspection of the HSV recordings where shearing of foam can be observed as small local and temporal deviations from the mean bubble motion at the pipe wall. These deviations are due to bubbles exchanging neighbours during shearing. Such deviations were observed only if the wall shear stress exceeded a certain limiting value that depends on

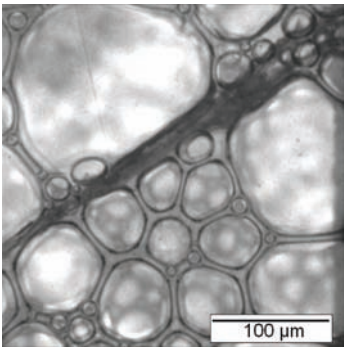

Figure 9. A microscopic image of a natural fibre in aqueous foam. Notice how the bubbles attach to the surface of the fibre.

foam properties. The values of the yield stress calculated by extrapolation of the fitted results in Figure 7 to 100% slip are prone to relatively large errors due to scatter in the experimental data which is limited to relative slip values below 40%. However, the qualitative behaviour is consistent with the most distinct findings from the HSV recordings; the yield stress increases with decreasing foam density and addition of hardwood fibres increases the yield stress considerably. The effect of rayon fibres and MFC on the yield stress is not so well-defined.

We can sum up, that at a selected consistency, the effect of fibrous material on the foam rheology depends on the characteristic length scale of fibres as compared with the mean bubble size as well as on the surface texture of fibres. Of the fibrous materials used in this study, the strongest impact was created by hardwood fibres, which have very rich surface texture, and the mean length that is one order of magnitude higher than the average bubble diameter. Reducing the characteristic fibre length to the mean bubble size (replacing hardwood fibres with MFC) or making the fibre surface smooth (rayon fibres) diminish the effect on the foam rheology. Especially surface texture has a high impact on the flow properties of fibre-laden foams.

CONCLUSIONS

The viscous behaviour of foams is generally described with a power law, and the addition of cellulosic particles did not change this general behaviour. Moreover, in all the cases the flow behaviour index was the same, namely $n = 0.6$. The solids, however, was found to have a significant effect on the consistency index and thus viscosity. The presence of natural wood fibres increased viscosity considerably, whereas for synthetic fibres of similar size the effect on foam viscosity was minimal. This difference could be explained by the difference in the strength of interaction between the fibres and bubbles. Microfibrillated cellulose also increased viscosity, but the effect was clearly smaller than that of natural fibres. While also having a strong interaction with bubbles MFC particles are much smaller and momentum transport is not as efficient as with natural fibres. Overall our results indicate that by applying the methodology described above on the data measured with one pipe diameter, one can calculate real material properties that are independent of boundary effects like slip velocity. This opens new possibilities for rheological analysis of particle foams, which so far has required rather complicated measurement setups.

ACKNOWLEDGEMENTS

We gratefully acknowledge Academy of Finland (project Fibre-Laden Foams), for supporting this work. We want also thank senior research technician Merja

Selenius for the photograph of the fibres (Figure 4, left and middle), and research scientist Ahmad Al-Quararah and Dr. Atsushi Tanaka for the photograph of a fibre in foam (Figure 9).

REFERENCES

1. B. Radvan and A. P. J. Gatward, The formation of wet-laid webs by a foaming process, *TAPPI*. **55** (1972) 748.
2. M. K. Smith, V. W. Punton and A. G. Rixson, The structure and properties of paper formed by a foaming process, *TAPPI*. **57** (1974) 107–111.
3. V. W. Punton, "The use of an aqueous foam as a fibre-suspending medium in quality papermaking." Foams: Proceedings of a symposium organized by the Society of Chemical Industry, Colloid and Surface Chemistry Group, in Academic Press, 1975: p. 179.
4. E. Kenttä, K. Kinnunen-Raudaskoski and T. Hjelt, Characterization of thin pigment coating layers produced by foam coating, *Tappi J.* **13** (2014).
5. K. Kinnunen-Raudaskosko, T. Hjelt, E. Kenttä and U. Forsström, Thin coatings for paper by foam coating, *Tappi J.* **13** (2014).
6. Ahmad M. Al-Qararah, A. Ekman, T. Hjelt, J. Ketoja, H. Kiiskinen, A. Koponen and J. Timonen, A unique microstructure of the fiber networks deposited from foam-fiber suspensions, *Colloids and Surfaces A: Physicochemical and Engineering Aspects* **482** (2015) 544–553.
7. Ahmad M. Al-Qararah, Tuomo Hjelt, Antti Koponen, Ali Harlin and Jukka A. Ketoja, Response of wet foam to fibre mixing, *Colloids and Surfaces A* **467 20** (2015) 97–106.
8. J. Lehmonen, Potential of foam-laid forming technology in paper applications, *Nord. Pulp Pap. Res. J.* **28** (2013) 392–398. doi:10.3183/NPPRJ-2013-28-03-p392-398.
9. A. Madani, S. Zeinoddini, S. Varahmi, H. Turnbull, A.B. Phillion, J.A. Olson, *et al.*, Ultra-lightweight paper foams: processing and properties, *Cellulose*. **21** (2014) 2023–2031. doi:10.1007/s10570-014-0197-3.
10. I. Mira, M. Andersson, L. Boge, I. Blute, G. Carlsson, Kristian Salminen, Timo Lappalainen and Karita Kinnunen, Foam forming revisited, Part I. Foaming behaviour of fibre-surfactant systems, *Nordic Pulp and Paper Research Journal*. **29** (2014) 679–688.
11. Timo Lappalainen, Kristian Salminen, Karita Kinnunen, Marjo Järvinen, I. Mira, M. Andersson, Foam forming revisited Part II. Effect of surfactant on the properties of foam-formed paper products, *Nordic Pulp and Paper Research Journal*. **29** (2014) 689–699
12. A. Savolainen, H. H. Mikkonen, P. Forssel and A. Suurnäkki, "Potential of wood fibres and nanoparticles in light-weight foams". Proceedings o TAPPI International Conference on Nanotechnology for the Forest Product Industry, in TAPPI Int. Conf. Nanotechnol. For. Prod. Ind., 2010.
13. S. Lapidot, "Nano Crystalline Cellulose Composite Foams From Renewable Resources". Proceeding of International Conference on Nanotechnology for Renewable Materials, in: Int. Conf. Nanotechnol. Renew. Mater., 2011.

14. Antti Koponen, Katariina Torvinen, Ari Jäsberg, and Harri Kiiskinen, Foam forming of long fibers, *Nordic Pulp & Paper Research Journal* **16**(2): pp. 239–247, 2016. doi: 10.3183/NPPRJ-2016-31-02-p239-247
15. H. Sehaqui, Q. Zhou and L. A. Berglund, High-porosity aerogels of high specific surface area prepared from nanofibrillated cellulose (NFC), *Compos. Sci. Technol*. **71** (2011) 1593–1599. doi:10.1016/j.compscitech.2011.07.003.
16. N. N. Thondavadi and R. Lemlich, Flow properties of foam with and without solid particles, *Ind. Eng. Chem. Process Des. Dev.* **24** (1985) 748–753. doi:10.1021/i200030a038.
17. Ari Jäsberg, Pasi Selenius and Antti Koponen, Experimental results on the flow rheology of fiber-laden aqueous foams, *Colloids and Surfaces A: Physicochemical and Engineering Aspects* **473**, (2015), 147–155. Doi: 10.1016/j.colsurfa.2014.11.041
18. H. Cui and J. R. Grace, Flow of pulp fibre suspension and slurries: A review, *Int. J. Multiph. Flow* **33** (2007) 921–934. doi:10.1016/j.ijmultiphaseflow.2007.03.004.
19. B. Herzhaft, S. Kakadjian and M. Moan, Measurement and modeling of the flow behavior of aqueous foams using a recirculating pipe rheometer, *Colloids Surfaces A: Physicochem. Eng. Asp.* **263** (2005) 153–164. doi:10.1016/j.colsurfa.2005.01.012.
20. S. Larmignat, D. Vanderpool, H. K. Lai and L. Pilon, Rheology of colloidal gas aphrons (microfoams), *Colloids Surfaces A Physicochem. Eng. Asp.* **322** (2008) 199–210. doi:10.1016/j.colsurfa.2008.03.010.
21. a. Saint-Jalmes, D. J. Durian, Vanishing elasticity for wet foams: Equivalence with emulsions and role of polydispersity, *J. Rheol. (N. Y. N. Y)* **43** (1999) 1411. doi:10.1122/1.551052.
22. Timo Lappalainen, Determinations of bubble size distribution of foam-fibre mixture using circular hough transform, *Nord. Pulp Pap. Res. J.* **27** (2012) 930–939. doi:10.3183/NPPRJ-2012-27-05-p930-939.
23. K. Niskanen, *Paper Physics* (2nd edn), Paperi ja Puu Oy, Helsinki, Finland, 2008.
24. R. J. Kerekes and C. J. Schell, Characterization of fibre flocculation regimes by a crowding factor, *J. Pulp Pap. Sci.* **18** (1992) 32–38.
25. M. Mooney, Explicit formulas for slip and fluidity, *J. Rheol. (N. Y. N. Y)* **2** (1931) 210. doi:10.1122/1.2116364.
26. F. A. Morrison, *Understanding Rheology*, New York; Oxford University Press, 2001, n.d.
27. B. S. Gardiner, B. Z. Dlugogorski and G. J. Jameson, Prediction of pressure losses in pipe flow of aqueous foams, *Ind. Eng. Chem. Res.* **38** (1999) 1099–1106. doi:10.1021/ie980385i.
28. C. Enzendorfer, Pipe viscometry of foams, *J. Rheol. (N. Y. N. Y)* **39** (1995) 345. doi:10.1122/1.550701.
29. T. Ralambotiana, R. Blanc and M. Chaouchea, Viscosity scaling in suspensions of non-Brownian rodlike particles, *Phys. Fluids* **9** (12), December 1997.
30. A. Laitinen, "Kuitususpension painehäviö suorassa putkessa" (special work), University of Jyväskylä, Finland, 1999.
31. Sanna Haavisto, Martina Lille, Johanna Liukkonen, Ari Jäsberg, Antti Koponen and Juha Salmela, "Laboratory-scale pipe rheometry: A study of a micro-fibrillated cellulose suspension", Proceedings of Papercon 2011, 1–4.5.2011, Northern Kentucky Convention Center, One West River Center Blvd., Covington, KY 41011.

Transcription of Discussion

THE EFFECT OF FIBROUS MATERIALS ON THE RHEOLOGY OF AQUEOUS FOAMS

Ari Jäsberg, Pasi Selenius and Antti Koponen

VTT Technical Research Centre of Finland Ltd, P.O. Box 1000, FI-02044 VTT, Finland

Paul Krochak RISE Bioeconomy

Do you have any estimates of the sheer profile? So you say there is a slip velocity and a bulk velocity. Are we talking about one bubble layer thick and then you jump up into the average velocity, or is there some sort of a defined profile?

Ari Jäsberg VTT Technical Research Centre

The slip velocity takes place in the thin liquid layer between the outer most bubble layer and the pipe wall. There is pure liquid drawn from the lamellae between the bubbles to the wall. That is the kind of well-established, well-accepted explanation for the formation of this layer.

Paul Krochak

So, my question is if we take it, bubble layer by bubble layer, what would the next bubble layer be doing? Is that already at the average velocity? So for example, you showed some numbers, 0.4 m/sec slip velocity, and then you had average velocity 0.12 m/sec, how thick is that? How rapid is that?

Ari Jäsberg

I have not calculated those, but I think based on those exponents, it is not very thin. I cannot give exact numbers on it at the moment.

Discussion

Gil Garnier Monash University

Very interesting. Why does the hardwood fibre have the most effect? What is the independent variable?

Ari Jäsberg

What is the reason for the effect of the hardwood fibre? Okay. I think that the reason is which I tried to point out in the conclusions slide, they are long enough and they have a rich surface texture on which the bubbles can attach, so they kind of glue nearby bubbles together. Therefore the adjacent bubble layers cannot move so freely next to each other because there are fibres in there and they are going through several bubble layers.

Gil Garnier

You have a three phase system, basically you have water, air and solid fibres with different roughness and a surfactant? Would the wetability play a key role in your phenomena?

Ari Jäsberg

Well I don't know about the detailed interaction between the fibres and the bubbles. It may have some effect there, but we have seen an effect on the slip velocity, because in some cases we have had a non-wetting case at the pipe wall. So we have just a stationary air bubble layer sitting at the pipe wall which kills the slip velocity totally. But to be frank, I have not studied the fibre bubble and the microscopic interaction myself, I cannot answer that; there may be some effect of course.

Gil Garnier

Where I am trying to go is, is it the physical chemistry of the interface, or is it the mechanical properties of the fibres that drives the phenomenon? There is an interesting experiment you can easily do with Lyocell fibres of different denier to characterize the effect of fibre flexibility. Have you tried?

Ari Jäsberg

Yes, in fact, we have started a new project in which one topic is to look more thoroughly at the effect of details of the fibre bubble interaction, what is the effect

if we change the fibre properties, how it will change the interaction with the bubbles and thereby rheology. That is something we are going to look at.

Daniel Söderberg KTH Royal Institute of Technology

So, one thing is the interaction between bubbles and fibres, but thinking about the results by Klingenberg and also later results by Bennington. What is the effect of fibre–fibre interactions since floculation is driven by fibre–fibre friction.

Ari Jäsberg

I think that the fibre–fibre interactions are the same if the fibres move in the water phase, but it seems that in the foam case, there is less chance for fibre–fibre interactions because fibres are somehow confined by the bubbles. The fibre–fibre interactions are not that frequent as in the water case.

Wenhao Shen State Key Laboratory of Pulp & Paper Engineering

In your experimental set up, you use a camera. I am wondering about the specification of the camera, the speed and the resolution.

Ari Jäsberg

We used a camera that has the capability of 1,000 frames per second.

Wenhao Shen

So it is a high-speed camera?

Ari Jäsberg

Yes, it is a high-speed camera.